Journal of Equine Veterinary Science 121 (2023) 104195

Contents lists available at ScienceDirect

Journal of Equine Veterinary Science

journal homepage: www.j-evs.com

Original Research Papers

Comparison of Six Different Methods for Measuring the Equine Hoof and Recording of its Three-Dimensional Conformation

Lina Sellke[a,*], Bianca Patan-Zugaj[a], Eberhard Ludewig[b], Robert Cimrman[c], Kirsti Witter[a]

[a] Department of Pathobiology, Institute of Morphology, Workgroup Anatomy, University for Veterinary Medicine, Vienna, Austria
[b] Clinical Division of Diagnostic Imaging, Department of Small Animals and Horses, University for Veterinary Medicine, Vienna, Austria
[c] New Technologies Research Centre, University of West Bohemia, Pilsen, Czech Republic

ARTICLE INFO

Article history:
Received 8 September 2022
Received in revised form 13 December 2022
Accepted 13 December 2022
Available online 17 December 2022

Keywords:
Horse
Hoof shape
Measurement
MicroScribe
Biometry

ABSTRACT

Different measuring techniques have been used to objectify the classification of hoof shape. The MicroScribe is a novel tool that might prove useful for measuring hooves without prior reconstruction or compensation of projection artefacts. The aim of this study was to compare biometric data of the equine hoof collected by the MicroScribe tool and measurements collected directly from hooves, scaled photographs and radiographs, from photogrammetry models and computed tomography datasets. The suitability of MicroScribe generated data to differentiate individual hoof conformations was tested. A total of 62 measures were recorded from 16 forehooves. 21 linear and nine angular measures were collected by at least four methods each, and evaluated further by analysis of variance (ANOVA) and multivariate analysis of variance (MANOVA). Ratios and differences of these measures were calculated as suitable for the definition of hoof shapes and analysed as well. Absolute equivalency of methods was detected for five linear and none of the angular measurements. The precision of the tested measurement methods was comparable. In some cases, different methods measure different structures. Radiographs tended to overestimate, while computed tomography slides to underestimate distances. Photogrammetry and scaled photographs were less suitable for measuring hoof angles. The MicroScribe tool can readily be used for hoof measurements. Its values for linear measures showed good equivalency with other methods based on real hooves. For angular measurements, the uneven hoof surface might introduce imprecision. Not all hoof conformations could be detected based on measuring results alone. Diagnosis by a skilled veterinarian is still essential.

1. Introduction

The determination of limb and hoof conformation by visual assessment is part of every orthopedic examination in equine medicine. This subjective classification can be supplemented by the use of objective measurements.

The relevance of these measures has already been demonstrated in a number of publications. Kane et al. [1] demonstrated that the risk for cannon bone fractures is lower when the toe angle is increased. Changes in shape parameters and hoof wall strain during a four week exercise program were shown by a study of Bellenzani et al. [2]. Previous studies also explored the relationship between standard hoof measurements and the hoof balance [3].

There are a number of objective methods available for the evaluation of the hoof conformation that are suitable and have already been used to determine the shape of the hoof.

Defined distances and angles can be measured directly on the hoof itself by ruler, caliper, protractor and tape measure. The measurements can be taken on anatomical specimens [4,5] or directly from hooves of living horses [6]. Direct measurements were used to evaluate the external surface of the hoof, some authors even took 30 single measurements or more [7,8], others have only taken one and examined it in relation to other measurements or diseases [9,10].

Distances and angles can also be collected from scaled photographs of equine hooves. For this technique, orthogonal photographs are made in different views with a scale bar at the same level as the prospective landmarks of measurement [11]. For every level to measure, it is necessary to take a separate photograph and to position the scale bar appropriately. Values recorded from the

Conflict of interest statement: The authors declare no conflicts of interest.

Animal welfare/ethical statement: Consent and approval were obtained from the horse owners, declaring the cadavers may be used for scientific research and teaching.

* Corresponding author at: Lina Sellke, Dr. med. vet., Institute of Morphology, Workgroup Anatomy, Veterinärplatz 1, 1210, Wien.
E-mail address: lina.sellke@vetmeduni.ac.at (L. Sellke).

https://doi.org/10.1016/j.jevs.2022.104195

photographs have to be recalculated in order to represent real life measures. This technique was used to investigate differences between lame horses and animals with normal gait [12] or changes in the hoof shape in response to exercise [13].

Measures of internal as well as external hoof structures can also be taken from standard radiographs of the hoof. Depending on the diagnostic question, plain radiographs [14] or radiographs after application of markers as barium sulfate -paste or metal bars [15] can be used. Structures on digital radiographs can be measured using DICOM software tools. For radiographic examinations of equine hooves, standards for recording and measuring have been developed [16]. Interobserver comparability and accuracy for standardized measurements in hoof radiographs in lateromedial and dorsopalmar direction have been assessed by Cripps and Eustace [17], and Kummer et al. [18].

Methods based on three-dimensional (3D)-reconstructions, for example, photogrammetry, computed tomography (CT) and magnetic resonance imaging (MRI) are also suitable for measuring distances and angles. Photogrammetry requires photographs of the object in a number of angles, so that each landmark used for alignment is clearly visible in at least two images. 3D models are created with specialized commercial or non-proprietary software. Labens et al. [19] validated this method for calculations of the hoof volume in comparison with CT volume measurements. The photogrammetry technique was also used for clinical research, such as a deformation study of equine hooves [20].

CT and MRI are methods based on the acquisition of cross-sectional images: Both are used routinely in veterinary radiology. The techniques have been successfully applied in equine hoof studies [19,21,22,23]. Medical software is used for reconstructing hoof structures and acquisition of measurements.

Except for direct measuring, all these methods share the necessity of the intermediate step "reconstruction" before measurements can be taken. This intermediate step entails the risk of distortion and data loss.

A novel tool that might prove useful for taking measurements of the hoof without the necessity of prior reconstruction, is the MicroScribe tool (Solution Technologies, Inc., Oella, MD), a portable measuring device with a flexible arm to collect surface coordinates by touching the object. This method has already been used for quantitative anatomical research in humans [24–27]. For horse studies, the MicroScribe has been used only rarely [28]. Hanley [29] applied this tool for his study on elastomeric hoof boots, however, the desired generation of a surface rendered 3D-model was unsuccessful. To our knowledge, the direct generation of quantitative data describing the equine hoof shape using the MicroScribe tool has not yet been validated and compared with other methods that are generally used for hoof measurements.

Therefore, the aim of this study was to compare biometric data of the equine hoof collected by the MicroScribe tool with measurements collected directly from hooves, from scaled photographs and radiographs, as well as from 3D models generated by the photogrammetry technique and CT datasets. The suitability of MicroScribe generated data to differentiate individual hoof conformations will be tested.

The MicroScribe generated data sets of all analysed hooves will be provided to the research community [30].

2. Material and Methods

2.1. Hooves and Work Sequence

16 cadaver front limbs of horses that died or were euthanized for health reasons unrelated to this study at the University for Veterinary Medicine in Vienna were used. The owners provided a declaration of consent that the cadavers may be used for scientific research and teaching.

A total of 62 hoof measures (complete list see Suppl.1) was taken for this project by L.S.. Six different methods were employed to collect the measurements. Measures that could be detected by at least four methods were analyzed in detail (Table 1). The names used for the individual measures were established according to Sellke et al., 2020 [31].

Additionally to the measures collected from the hooves, a number of ratios and differences that are supposed to describe different hoof conformations were calculated: Frog width/Frog length ratio [11], Hoof width/Weight-bearing length ratio [32], Dorsal hoof wall length/Heel length ratio [12], Dorsal coronary band height/Heel height ratio [15], Dorsal hoof wall angle/Heel angle ratio [33], Lateral-Medial heel length difference [34], Lateral-Medial heel height difference [35], Lateral-Medial hoof wall length difference [35], Lateral-Medial hoof width difference [34], Lateral-Medial heel angle difference [34] and Lateral-Medial lateral hoof wall angle difference [35].

All hooves were examined by an experienced orthopedist (B.P.Z.), their conformation was determined subjectively. The procedure for visual assessment of the hoof shape can be found in Supplement 1. The hooves were classified based on their conformation distinguishing hooves with and without the conformation of interest (Supplement 1). One hoof could therefore be listed in several groups, as the different conformations were examined individually.

Limbs were stored frozen in plastic bags at -20°C.

2.2. Terminology

The six measuring methods employed in this study, names of the measures and of the hoof conformations will be capitalized in the following text to facilitate readability. The methods will be designated as follows with the intention to clearly distinguish the method from the device or object with which or on which the measurements are made: Direct measurements, Scaled photographs, Microscribe, Photogrammetry, Radiography, and CT (for detailed description see 2.3.).

2.3. Measuring Methods

The frozen hooves were subjected to Direct measurements, digitized with the MicroScribe tool and photographed for Scaled photography and Photogrammetry. Afterwards, the hooves were stored overnight at 4°C to ensure gentle thawing. The second day, CT scanning was performed and radiographs were taken.

2.3.1. Direct Measurements

The roughly cleaned, still frozen hooves were fixed with two clamps on a flexible stand. With ruler, measuring tape, protractor and caliper, 24 linear and seven angular measures were taken on every hoof with an accuracy of 0.1 mm or 0.5 degrees.

2.3.2. Scaled Photographs

A digital compact system camera (Casio ex-zr100, (Casio Computer Co., Ltd, Tokyo-Shibuya, Japan), focal length 4.24 to 53.0 mm, autofocus) was used. After positioning of a paper scale bar as described below, four photographs were taken of each hoof: Two in lateral view from both sides, with the scale bar in the axial plane, one in solear view with the scale bar at the level of *Margo solearis* and one photograph in dorsal view, the scale bar being positioned at the level of the widest part of the hoof. Each photograph was taken with the hoof positioned in the center of the image. The distance between camera and hoof center was 20 cm. The zoom

Table 1
Names and definitions of the analyzed measures [31].

Name of the Measure	Definition	Measuring Methods
Weight-bearing length	Length of *Facies contactus* of *Facies solearis*	Dm, Sp, Ms, Pg, Rg, CT
Hoof width	Linear distance between the widest part of *Pars lateralis/medialis*	Dm, Sp, Ms, Pg, Rg, CT
Lateral/Medial hoof width	Linear distance between the sagittal axis and the widest part of *Pars lateralis/medialis*	Dm, Sp, Ms, Pg, Rg, CT
Dorsal hoof wall length	Linear distance from the most dorsoproximal point of *Pars dorsalis, measured* along the hoof wall to the ground line	Dm, Sp, Ms, Pg, Rg, CT
Lateral/Medial hoof wall length	Linear distance between the most dorsolateral/-medial point of *Margo coronalis* and the ground line, measured along the hoof wall of *Pars lateralis/medialis*	Dm, Sp, Ms, Pg, Rg, CT
Lateral/Medial diagonal hoof length	Linear distance between the most dorsodistal extent of *Pars dorsalis* and the curved palmar end of *Pars inflexa lateralis/medialis* at *Facies solearis*	Dm, Sp, Ms, Pg
Heel length	Linear distance between the most palmarolateral/-medial and most distal part of *Pars mobilis lateralis/medialis*	Dm, Sp, Ms, Pg, CT
Heel height	Vertical distance between the most palmarolateral/-medial part of *Pars mobilis lateralis/medialis* and the ground line	Dm, Sp, Ms, Pg, CT
Heel width	Linear distance between the palmarolateral and palmaromedial end of *Facies contactus* of *Facies solearis*	Dm, Sp, Ms, Pg
Frog width	Linear distance between the most palmarolateral and palmaromedial end of *Cuneus ungulae*	Dm, Sp, Ms, Pg
Frog length	Shortest linear distance between *Apex cunei* and the line connecting the palmar ends of *Cuneus ungulae*	Dm, Sp, Ms, Pg
Frog to tip	Linear distance between the most dorsodistal extent of *Pars dorsalis* and *Apex cunei*	Dm, Sp, Ms, Pg, Rg
Bulb distance	Transverse distance between the most convex parts of *Torus ungulae*	Dm, Sp, Ms, Pg
Dorsal coronary band height	Vertical distance between the most dorsoproximal point of *Margo coronalis* and the ground line	Dm, Sp, Ms, Pg, Rg, CT
Coronary band length	Projected length of *Margo coronalis* in lateromedial aspect, measured between the most dorsoproximal and palmarodistal point	Dm, Sp, Ms, Pg, Rg, CT
Coronary band width	Distance between the most lateral and most medial part of *Margo coronalis*	Dm, Sp, Ms, Pg, Rg, CT
Lateral/Medial hoof wall angle	Angle of *Pars lateralis/medialis* of the hoof wall and the ground line	Dm, Sp, Ms, Pg Rg, CT
Lateral/Medial proximal hoof wall angle	Angle of the proximal third of *Pars lateralis/medialis* and the ground line	Sp, Ms, Rg, CT
Lateral/Medial heel angle	Palmar/plantar angle between *Pars mobilis lateralis/medialis* and the ground line	Dm, Sp, Ms, Pg, CT
Dorsal hoof wall angle	Angle between *Pars dorsalis* of the hoof and the ground line in palmar/plantar direction	Dm, Sp, Ms, Pg, Rg, CT
Coronary band angle	Angle between *Margo coronalis* and the ground line in lateral aspect	Dm, Sp, Ms, Pg, Rg, CT
Mediolateral symmetry	Angle between a line parallel to *Margo coronalis* and the ground line in dorsal aspect; Angle between *Facies articularis* of *Phalanx distalis* and the ground line in dorsopalmar view	Ms, Pg, Rg, CT

Abbreviations: CT, computed tomography; Dm, direct measurements; Ms, microscribe; Pg, photogrammetry; Rg, radiography; Sp, scaled photographs.

function of the camera was not used, resulting in a wide-angle setting of 24 mm focus length (35 mm equivalent). The photographs were printed in A4 in the original side ratio, and 21 linear and eleven angular measures per hoof were taken from each set of photographs with a standard ruler and a protractor with an accuracy of 0.5 mm or 0.5 degrees. The linear dimensions were converted individually for each photograph using the rule of proportions based on the scale bar.

2.3.3. Microscribe

For the Microscribe method, the hoof surface was digitized using the MicroScribe G (Solution Technologies, Inc., Oella, MD), the MicroScribe Utility software provided by the producer, which allows the recording of datapoint coordinates immediately into Microsoft Excel (Microsoft Corporation, WA). The frozen limbs were fixed on a bench vice with a mounting arm and two clamps the sole directed upwards so that the hoof wall could be reached with the MicroScribe probe from beneath. Before starting the landmark recording, three needle pins were positioned at the most dorsal, lateral, and medial point of *Facies solearis* for easier orientation. The xyz-coordinates of 73 points per hoof were recorded and automatically transferred into an Excel document.

The hoof measurements were generated from the point coordinates by a custom software (R.C.) [36]. The software, called "hoofstats," is freely available and can be found at https://gitlab.com/hoofstats/hoofstats, where the sources, installation instructions and examples of use are provided. It can read directly the Excel data sets [30] and uses a simple domain-specific language (DSL) to describe the geometrical entities defined using the Microscribe point cloud coordinates and their mutual relations. For example, the following entries

```
...
'_line1' : ('line', 'HW_0_prox', 'HW_0_dist'),
'_plane1' : ('plane', 'FS_0_marg',
'FSR_135_marg', 'FSL_135_marg'),
'_i2' : ('intersect-line-plane', '_line1',
'_plane1'),
'f' : ('segment', 'HW_0_prox', '_i2'), ...
```

define a line ('_line1′) using two points from the point cloud, a plane ('_plane1′) using three points, compute a new point ('_i2′) at the intersection of the line and plane and finally a segment ('f') on the line using the computed point and a point existing in the dataset. The full DSL description of the hoof measures can be found at [30]. The software evaluates this description using a built-in geometrical engine and outputs (as an Excel file) the measures of the various geometrical entities. Optionally, it can also visualize selected entities, such as in Fig. 1, which corresponds to the entities in the above example.

2.3.4. Photogrammetry

For photogrammetry, the frozen limbs were fixed upside down on a bench vice with a mounting arm and two clamps. The limbs were positioned in the middle of a well-lit room with little natural light. Shadows were eliminated as far as possible. A paper scale was fixed on the sole, away from structures later to be measured. By leaving the limb in the exact same position, 50 photographs of the hoof were taken from all sides, at different angles and different distances, one of them orthogonal to the scale on *Facies solearis*. Photographs were transferred to a personal computer and

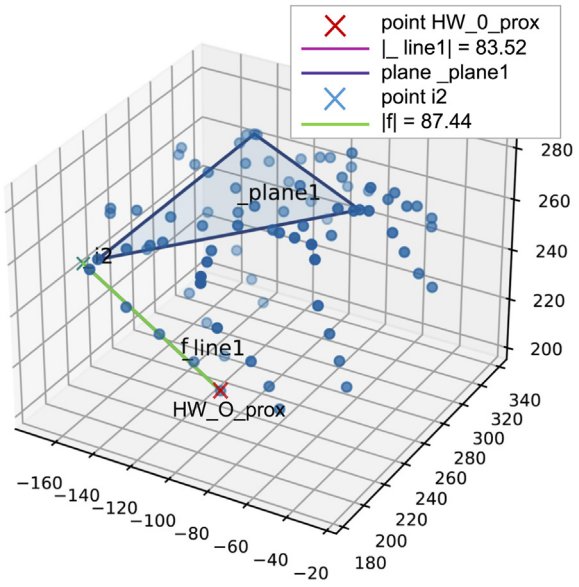

Fig. 1. Visualization of point vectors of the hoof surface (blue dots) and of selected geometrical entities representing the measure Dorsal hoof wall length (f). The distance f (in this example 87.44 mm) goes from point HW_o_prox to the reconstructed point i2, the intersection between plane1 (virtual reference plane – weight-bearing margin) and line1, a straight along the dorsal hoof wall, according to the definition of the measure. (Sellke et al., 2020). X-, y- and z-axis are given in mm. Line1 (purple) is covered by f (green) in this projection. (For interpretation of the references to color in this figure legend, the reader is referred to the Web version of this article.)

loaded to the free basic version of the photogrammetry software 3DF Zephyr (3DFlow, Udine, Italy). This program allows 3D modeling and measuring of the model after calibration using the photographed scale. Twenty-one linear and seven angular measures were taken, using the provided tools. For two additional measures (Lateral and Medial hoof wall angle) a virtual protractor [37] was applied.

2.3.5. Radiography

Radiographs of the hooves were acquired using an X-ray machine for large animals (Super 100 CP, PHILIPS Healthcare, Hamburg, Germany). Images were recorded with a digital flat-panel detector (FDR D-EVO II C24 Fujifilm, Tokyo, Japan). The limbs were mounted on a stand to mimic the position in loaded condition.

Exposure settings were 60 kVp and 10 mAs. The resulting S-value, the exposure indicator of the system, was in a range of 400 ± 40. Other constant exposure parameters were a focal spot size of 1.2 × 1.2 mm^2, a focus to object distance of 100 cm, a total filtration of 2.0 mm Aluminum and no anti-scatter grid usage.

Two radiographs were taken of each hoof. For the first radiograph (lateromedial view), the most dorsoproximal and palmarodistal points of the coronary band were marked with barium sulfate-paste (the palmarodistal point at the heel closer to the image detector), the tip of the frog with a metal marker. The radiographs were recorded with the central beam tilted by 1 to 2 degrees. The second radiograph was taken in dorsopalmar view, with additional barium sulfate-markers laterally and medially at the widest part of the coronary band. The marking technique was adapted after [16,18].

The radiographs were exported in DICOM-format and analyzed on a radiological workstation (JiveX; VISUS Health IT GmbH, Bochum, Germany). 29 linear and 16 angular measures were recorded using the distance and angle measurement tools. Landmarks for measurements (Table 1) were defined as described in detail before [31] after appropriate adjustments of brightness and contrast.

2.3.6. Computed Tomography

In order to avoid barium sulfate-caused artefacts, CT scanning was performed prior to radiography. A 16-slice helical medical scanner was used (Somatom Emotion 16; Siemens Healthcare, Erlangen, Germany). The limbs were kept in plastic bags during the procedure for sanitary reasons. The axis of the limb was concordant with the axis of the table (z-axis). Transverse CT scans were acquired at 130 kVp and 200 mA with a slice thickness of 0.6 mm, rotation time of 1 s and a pitch of 0.8. The field of view was 160 × 160 mm^2 with a scan matrix size of 512 × 512. The resulting voxel size was 0.3 × 0.3 × 0.6 mm^3 in x-, y- and z-axis, respectively.

Multidirectional images were reformatted from the transverse acquired datasets using medical workstation functionalities.

29 linear and 15 angular measurements were taken with the available distance and angle tools using a bone window setting (window width 3100 HU, window level + 500 HU) or a soft tissue window setting (window width 280 HU, window level + 50 HU) as appropriate.

2.4. Statistical Analysis

All statistical tests were conducted using the IBM SPSS Statistics v.28 software (International Business Machines Corp., Armonk, NY).

The six measuring methods were compared for each measure using the one-way repeated measure ANOVA after testing normality of distribution (Shapiro-Wilk test, $\alpha = 0.05$) and homogeneity of variance (Levene's-test $P > .05$). The SPSS software provides immediately post hoc pairwise comparison results with Bonferroni correction so that $P < .05$ was set as the level of significance. Bland-Altman analysis was used to summarize the comparison for each pair of methods for all measures.

The suitability of Microscribe generated data to differentiate between individual hoof conformations was analyzed based on measures and their ratios and differences [11,12,15,32–35]. Differences, were converted to their absolute values, so that only positive numbers entered further analysis. One-way MANOVA was used to identify hoof measures distinguishing between hooves with the conformation of interest and all other hooves. Hoof conformation (yes/no) and hoof measures were set as group and dependent variable, respectively. Data sets were tested for normality of distribution (Shapiro-Wilk test, $\alpha = 0.05$), the correlation between the variables ($r < 0.90$), multivariate outliers (Mahalanobis distance), homogeneity of the error variances (Levene's-test $P > .05$) and homogeneity of covariances (Box's-test $P > .01$). If normality of distribution was not given, the test was run nevertheless, as one-way MANOVA is considered robust to violation of this assumption [38]. If the correlation between variables was too high, the according measures (mostly lateral and medial pairs) were cumulated and the mean was used, or the measure was excluded from analysis. If the homogeneity of error variances was too low ($P < .05$), Roys Largest Root was used instead of Wilks Lambda.

Since MANOVA requires more cases in each group ((i) hooves with conformation of interest; (ii) hooves without conformation of interest) than the number of analyzed dependent variables (Weight-bearing length, Hoof width, Dorsal hoof wall length...), measures were merged as appropriate (Mean instead of Lateral and Medial diagonal hoof length, heel length, heel height) and the analysis itself was split by measure groups, for each conformation individually.

After MANOVA, post-hoc univariate ANOVA was conducted for every measure. The level of significance was set at $P < .05$.

3. Results

A total of 42 linear and 17 angular measurements, as well as three areas was collected from hoof samples using the six methods: Direct measurements, Scaled photographs, Microscribe, Radiography, Photogrammetry and CT. The complete data set is provided in Supplement 1. For further analysis, we selected data that could be collected by at least four different methods. 21 linear and nine angular measures were included in the further analysis. Measures requiring bone landmarks did not qualify, since these technically could not be taken with methods relying on the hoof surface only (Direct measurements, Scaled photographs, Microscribe, Photogrammetry).

Some of the analyzed measures could not be collected by all six methods for a number of reasons: Artificial markers (barium sulfate, metal bars) could not be used for CT scanning due to shadow artifacts in reconstructed slices, rendering landmarks definition impossible for Lateral and Medial diagonal hoof length, Heel width, Frog length and width and Frog to tip. For Bulb distance, the definition of an appropriate section plane was nearly impossible in CT slices. For Lateral and Medial diagonal hoof length, Heel width, Lateral and Medial heel length, width, and angle, as well as for Bulb distance, the necessary landmarks could not be identified in radiographs, since the summation shadow of wider structures covered the structures of interest. The palmar landmark(s) for measuring Frog length and width were constructed virtually and thus could not be artificially marked for radiography. For Lateral and Medial proximal hoof wall angle, the protractor could not be positioned correctly onto whole (nonsectioned) hooves. Additionally, for these measures the necessary digital measuring tool for Photogrammetry was not at our disposal. The extremely small Mediolateral symmetry angle could not be collected in Scaled photographs for the large virtual distance of the angle vertex from the printouts.

Data were distributed normally and the assumption of homogeneity of variance was met, therefore, parametric tests (ANOVA) were used for further analysis.

For the purpose of this study, we have regarded nonsignificant differences between the methods for each single measures as an indicator for methods equivalency.

3.1. Linear Hoof Measures

Ten of the linear measures could be collected by all six methods, five by five methods and the remaining six by four methods. All methods provided homogeneous result with similar spread and few outliers. A comparison of methods for collecting linear measures is presented in Fig. 2. For five of the measures (Fig. 2E, F, I, M, V), no significant differences were detected between the methods ($P > .05$). However, three of these measures could only be collected by a subset of four methods (Fig. 2E, F, I; Direct measurements, Scaled photographs, Microscribe and Photogrammetry).

For many of the measures, values collected from radiographs were higher than those recorded using the other techniques (Fig. 2B, D, G, K, N, O; $P < .05$). In contrast, values recorded from CT slices were often systematically lower than the rest of the data set (Fig. 2Q, R, T, U, $P < .05$). A complete list of significance levels resulting from post-hoc pairwise comparison is given in Supplement 2. Bland-Altman plots comparing each pair of measuring techniques for all linear measures are summarized in Supplement 3A.

3.2. Angular Hoof Measures

A total of nine angular measures was analyzed in detail. Four of them could be measured by all six methods, two using five methods and three using four methods.

Angle measures generally produced less homogeneous results than linear measures; more outliers were identified. For all of the angle measures, significant differences have been detected between the single measuring methods ($P < .05$) (Fig. 3). None of the methods produced systematically higher or lower values for angle measurements. Bland-Altman plots comparing each pair of measuring techniques for all angular measures are summarized in Supplement 3B.

3.3. Comparison of Individual Measuring Methods

A complete list of probabilities of error (p-values corrected for alpha error) resulting from pairwise post-hoc comparisons between the measuring methods is given in Supplement 2. In general, a good equivalence for linear measures was detected between methods based on real hooves (Direct measurements, Microscribe, Scaled photographs, Photogrammetry; Table 2), where approximately 60% to80% of the analyzed measures could be collected by either method without producing significantly different results. In contrast, radiographic examination yielded equivalent results for less than 30% of the analyzed measures when compared with Direct measurements, Microscribe, and Photogrammetry. Interestingly, the agreement of the results between Radiography and CT was comparably low.

For angular measures, CT showed good equivalence with Microscribe, Direct measurements, and Photogrammetry, but also with Radiography, whereas results collected from Scaled photographs were comparable with that from other methods for only approximately 30% of the analyzed measures (Table 2). For Frog width, pairwise post-hoc comparisons did not detect significant differences between the individual methods, although the ANOVA was significant at $P = .029$.

3.4. Microscribe in Comparison With Other Measuring Methods

The MicroScribe as a novel tool for capturing hoof measurements has been analysed separately, additionally to the general comparison of methods. For linear measures, the Microscribe method showed good equivalency with Direct measurements, Scaled photography and Photogrammetry (15, 14 and 14 of the 21 linear measures with no significant differences between methods). In contrast, when compared with Radiography, for all but three measures, differences between the methods were detected. For angular measures, the highest equivalency was detected between Microscribe and CT (seven of nine measures with no significant differences between methods) (Supplement 2).

Figs. 4 and 5 compare the values collected by the five established measuring methods with that recorded by Microscribe for 21 different linear and nine angular hoof measures. For linear measures, the data spread varied from less than 3% of the Microscribe value (Lateral and Medial diagonal hoof length) to more than 45% (Medial heel height). For angular measures, data differed between 11% (Dorsal hoof wall angle) and 66% (Mediolateral symmetry) from the Microscribe values. Despite the variance between the single measuring methods (see discussion on general method differences), Microscribe values, clustered with at least some of the other data, with the notable exception of Mediolateral symmetry.

3.5. Hoof Measurements and Hoof Conformation

The following conformations were found among the 16 hooves analysed for this study: Under-run heels (n = 9), Long toe (n = 5), Diagonal hoof (n = 8), Symmetric hoof (n = 5, in contrast to asymmetric hooves), Under-run/flair hoof (n = 6) Club hoof (n = 1) and Contracted heels (n = 2). The conformations Club hoof and Contracted heels could not be statistically evaluated due to the small

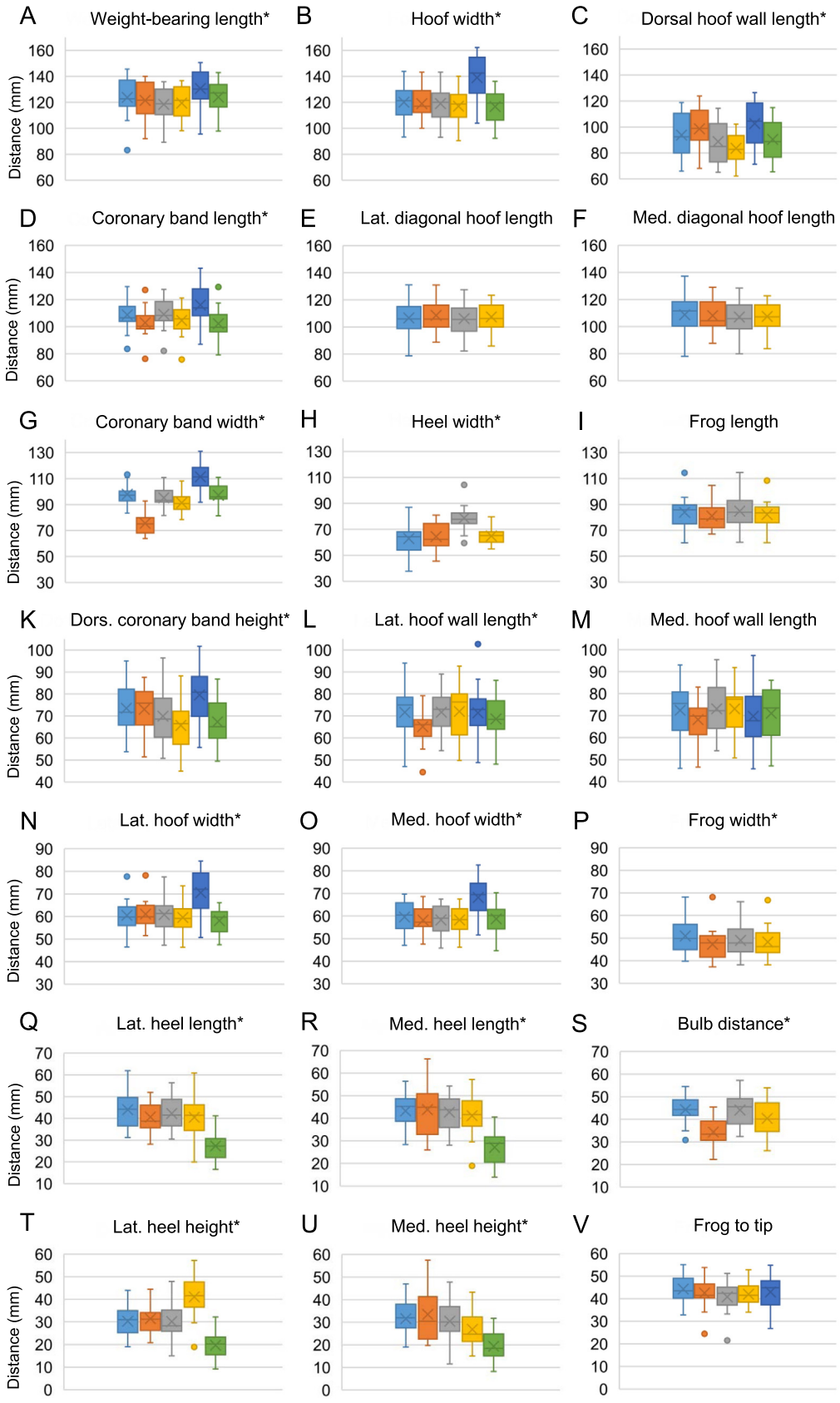

Fig. 2. Comparison of methods for collecting linear measures of the equine hoof. Methods are color coded: Light blue, Direct measurements; orange, Scaled photographs; grey, Microscribe; yellow, Photogrammetry; dark blue, Radiography; green, CT. Measures for which individual methods resulted in different values (one-way repeated measures ANOVA, $P < .05$) are marked with an asterisk. Lat. = lateral, med. = medial, dors. = dorsal. Boxes span the interquartile range of the datasets (n=16) on the y-axis in mm. The inside lines indicate the median and the × in the boxes the mean values. Whiskers extend to the minimum and maximum values excluding outliers (dots). (For interpretation of the references to color in this figure legend, the reader is referred to the Web version of this article.)

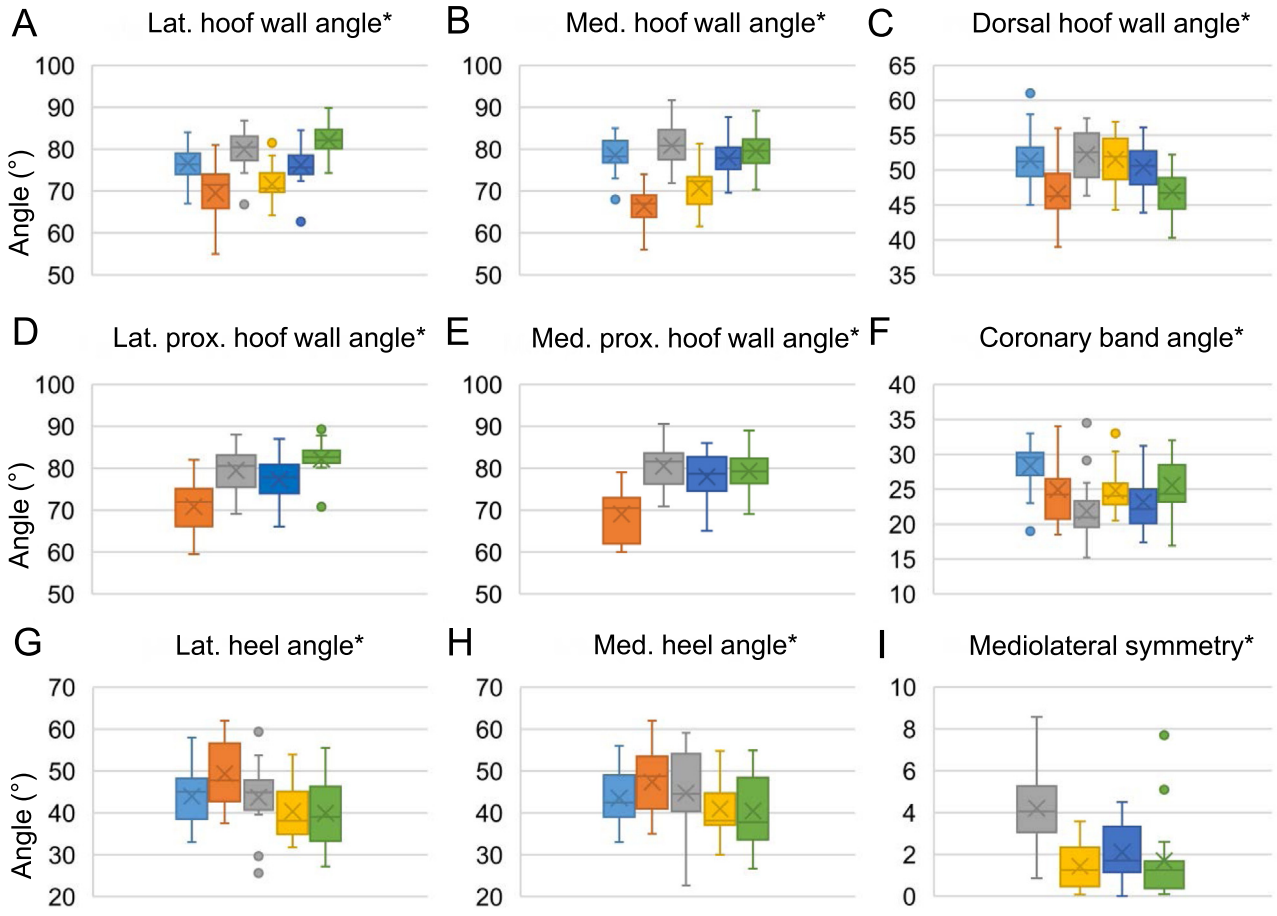

Fig. 3. Comparison of methods for collecting angular measures of the equine hoof. Methods are color coded: Light blue, Direct measurements; orange, Scaled photographs; grey, Microscribe; yellow, Photogrammetry; dark blue, Radiography; green, CT. Measures for which individual methods resulted in different values (one-way repeated measures ANOVA, P < .05) are marked with an asterisk. Lat. = lateral, med. = medial, prox. = proximal. Boxes span the interquartile range of the datasets (n=16) on the y-axis (in degrees). The inside lines indicate the median and the × in the boxes the mean values. Whiskers extend to the minimum and maximum values excluding outliers (dots). (For interpretation of the references to color in this figure legend, the reader is referred to the Web version of this article.)

Table 2
Equivalence of hoof measuring methods expressed by the number of measures for which no significant differences could be detected between results collected by either method (Tukey's post hoc test, $P > .05$ after alpha error correction).

Compared Methods	Number of linear Measures for Which Methods are Equivalent Per Total Number of Measures	Number of Angular Measures for Which Methods are Equivalent Per Total Number of Measures
Direct measurements vs. Scaled photographs	**17/21 (81.0%)**	2/6 (33.3%)
Direct measurements vs. Microscribe	**15/21 (71.4%)**	3/6 (50.0%)
Direct measurements vs. Photogrammetry	12/21 (57.1%)	3/6 (50.0%)
Direct measurements vs. Radiography	*3/11 (27.3%)*	**3/4 (75.0%)**
Direct measurements vs. CT	6/14 (42.9%)	**4/6 (66.7%)**
Scaled photographs vs. Microscribe	**14/21 (66.7%)**	*2/8 (25.0%)*
Scaled photographs vs. Photogrammetry	**14/21 (66.7%)**	2/6 (33.3%)
Scaled photographs vs. Radiography	4/11 (36.4%)	*1/6 (16.7%)*
Scaled photographs vs. CT	7/14 (50.0%)	*2/8 (25.0%)*
Microscribe vs. Photogrammetry	**14/21 (66.7%)**	3/7 (42.9%)
Microscribe vs. Radiography	*3/11 (27.3%)*	3/6 (50.0%)
Microscribe vs. CT	6/14 (42.9%)	**7/9 (77.8%)**
Photogrammetry vs. Radiography	*3/11 (27.3%)*	3/5 (60.0%)
Photogrammetry vs. CT	8/14 (57.1%)	4/7 (57.1%)
Radiography vs. CT	*3/10 (30,0%)*	**5/7 (71.4%)**

Bold: no significant differences for 60% or more of the analysed measures – equivalent methods; Italics: no significant differences for 30% or less of the analysed measures – nonequivalent methods.

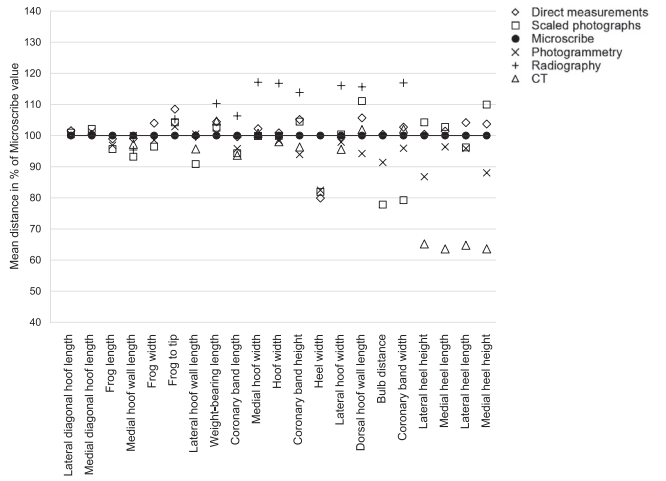

Fig. 4. Comparison of the Microscribe method for collecting linear hoof measurements (black dots) with five other methods, analyzing 21 linear measures. Results are given in % of the Microscribe values as calculated from the means of each measure (n=16). (For interpretation of the references to color in this figure legend, the reader is referred to the Web version of this article.)

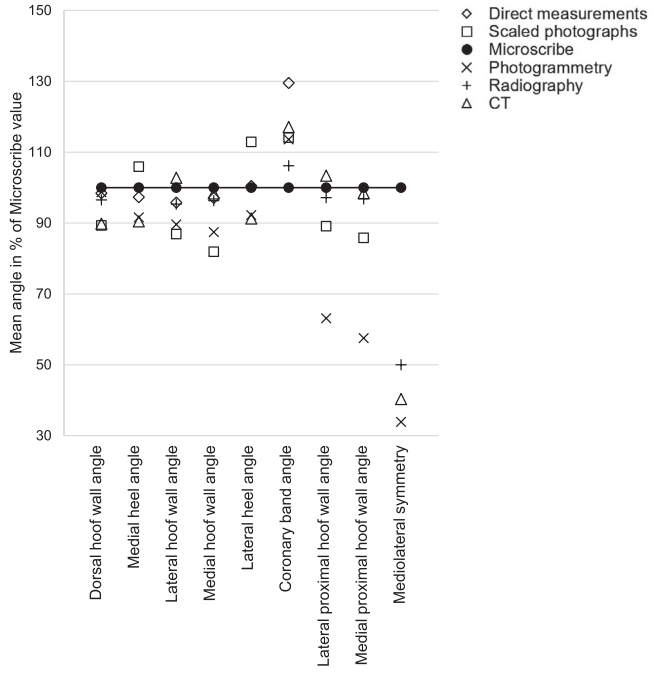

Fig. 5. Comparison of the Microscribe method for collecting angular hoof measurements (black dots) with five other methods, analyzing nine measures. Results are given in % of the Microscribe values as calculated from the means of each measure (n=16). (For interpretation of the references to color in this figure legend, the reader is referred to the Web version of this article.)

number of cases in the affected group. The conformation Underrun heels/flair hoof was not included in the analysis, since the data variability of the defining measure was too high. We based the further analysis of the hoof conformations on the Microscribe data.

Nine of the 16 samples were classified as hooves with Underrun heels. A set of 11 linear and six angular measures (including one difference between angles), as well as five ratios were analyzed for this conformation (Fig. 6) as to whether they discriminate between hooves with and hooves without under-run heels. Mean diagonal hoof length, Mean heel length, Mean heel height, Lateral and Medial hoof wall lengths and the ratio between Hoof width and Weight-bearing length, but none of the angle measures detected differences between the groups. Some further measures seemed to discriminate between the conformations (e.g., Dorsal hoof wall length, Dorsal coronary band height, Heel angle) but did not differ significantly.

Five of 16 samples were classified as hooves with Long toes. A set of 11 linear and five angular measures as well as five ratios were analyzed for this conformation (Fig. 7). For none of these measures, significant differences could be detected between hooves with and hooves without Long toes. Some measures seemed to discriminate between the conformations (e.g., Weight-bearing length, Dorsal hoof wall length, Dorsal coronary band height) but did not differ significantly.

Eight of the 16 samples were classified as Diagonal hooves. 14 linear and seven angular measures, as well as seven differences were analysed for this conformation (Fig. 8). Weight-bearing length, Hoof width and Dorsal hoof wall angle, as well as Mean heel angle (not shown), but none of the differences between lateral/medial measures discriminated between diagonal hooves and all other samples. Hoof width, Diagonal hoof length and Heel angle might discriminate between conformations but did not differ significantly in our data set.

Five of the 16 samples were classified as Symmetric hooves. A set of 15 linear and six angular measures, as well as six differences were analysed for this conformation (Fig. 9) as to whether they discriminate between Symmetric hooves and asymmetric hooves. Only the measure Weight-bearing length detected differences between the groups in our sample.

4. Discussion

4.1. Measuring Methods

Measurements for scientific and diagnostic purposes can be collected from equine hooves by different approaches and techniques [7,11,16,21]. It is usually tacitly presumed that the individual methods yield equivalent results [39,40]. However, the results of our study suggested that not for all measures the single methods can be regarded as interchangeable. For all angular and most of the linear hoof measures, significant differences could be detected between the data collected by the different approaches (Figs. 2 and 3). A recent study comparing 3D scanning, Photogrammetry and Direct measurements came to a similar conclusion regarding method equivalency [41].

Measures based on clear landmarks that are easy to find with all methods (e.g., Lateral and Medial diagonal hoof length, Frog length), tended to produce equivalent results irrespective of the used method. In contrast, for measures as Coronary band width or the Lateral/ Medial hoof wall angle, landmark definition was less easy. For Direct measurements and Microscribe and to a certain degree Photogrammetry, some of the landmarks had to be constructed in free space, for example the dorsodistal landmark of Dorsal hoof wall length and Weight-bearing length in hooves with rounded or broken wall, or the palmar landmark for Weight-bearing length in the axial plane.

Angle measures reacted more sensitively to small changes in the landmarks than linear measures. A minimum of three landmarks is required for angle definition. Small imprecisions can sum up to higher differences between the measured values.

Methods that introduced the largest general variance into the measurements were Radiography and CT for linear and Scaled photographs and Photogrammetry for angular measures.

(Linear) measurements taken from radiographs tended to be larger than those collected by other methods. This may be explained by the technical circumstances of how radiographs are taken as well as how they are measured. Radiographs are per-

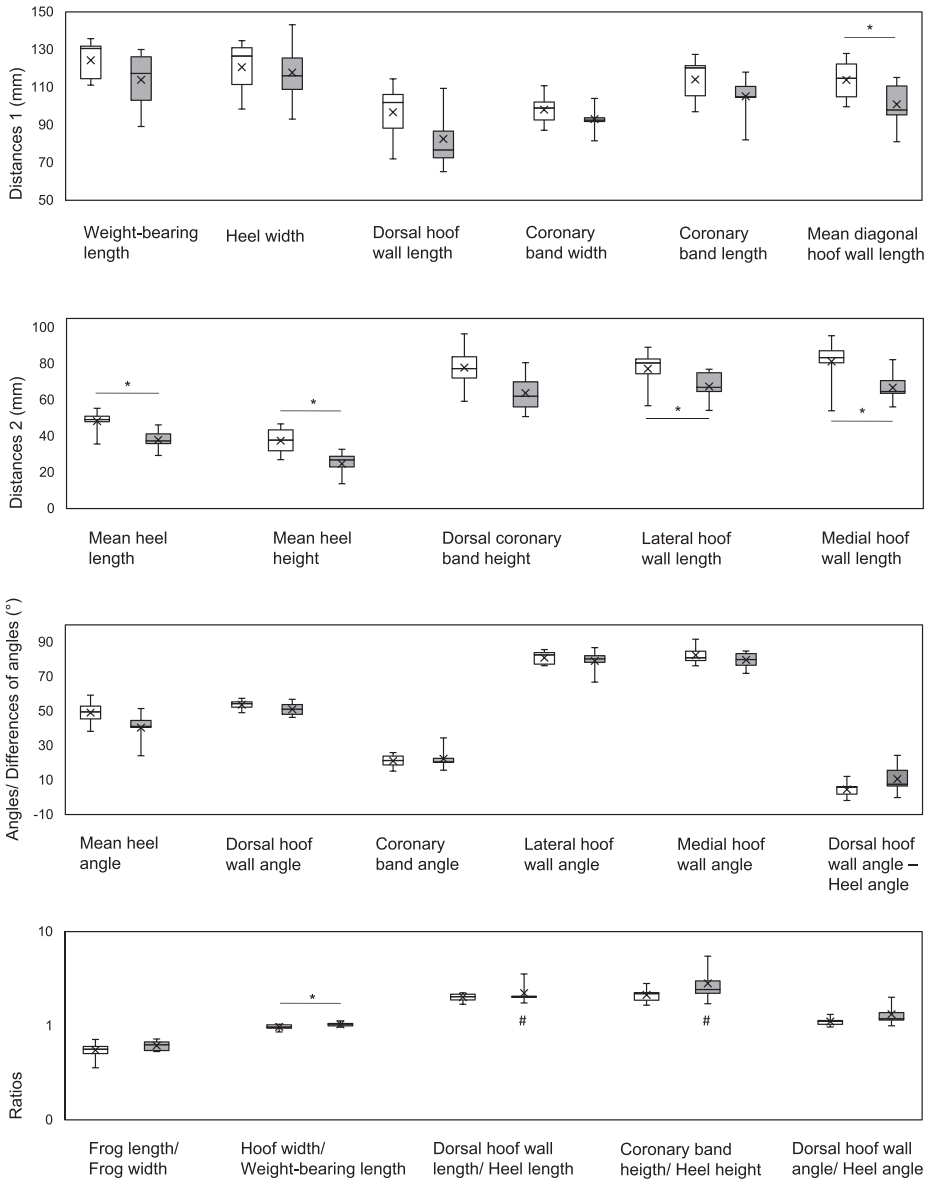

Fig. 6. Differences between measures of hooves without (white boxes, left side of the pairs) and with (grey boxes, right side) Underrun heels. Significant differences between hooves with Underrun heels and all other hooves were detected for five linear measures and one ratio (asterisks; post-hoc univariate ANOVA, $P < .05$). Boxes span the interquartile range of the measured values on the y-axis (n=16). The inside lines indicate the median and the × symbol mean values. Whiskers extend to the minimum and maximum values. Data sets that are not normally distributed are marked with a hash symbol. (For interpretation of the references to color in this figure legend, the reader is referred to the Web version of this article.)

spective projection images with X-rays diverging from the focus point to the detector [42–45]. As a result, structures of the object appear larger than in reality, especially if the structures of interest are distant from the detector (e.g., Hoof width, Coronary band length). Furthermore, the parallax effect has to be taken into account [46,47]. Shadow summation (e.g., Weight-bearing length, Heel length) due to overlap of structures in radiographs might make the identification of landmarks difficult, so that the maximum distance for example, between hoof tip and sole end may be overestimated.

In contrast, linear measurements recorded from CT image sets were often smaller than those collected by other methods. Depending on the measure, different explanations might apply: one central point was probably the definition of the virtual section plane in which the CT slice was reconstructed for measuring [48]. For example, for the Heel length measurement, an appropriate sagittal section plane was chosen. If the maximum extension of the heel is not situated in this plane but slightly oblique, its dimensions will be underestimated. Another example was the difficulty to find the widest point of the hoof in a chosen orientation when scrolling through a series of CT slices, whereas this task was easy in projection images such as radiographs or scaled photographs.

Scaled photographs seemed to be less suitable for angle measurement, since they produced data sets that were different to that of all other methods. A possible explanation might be the nonlinear distortion produced by camera lenses, which influences angles more severely than distances, especially when pictures are taken at a small distance from the object. It is known that distortion correction is crucial for any computer vision task [49–51]. In our case, no computational correction was used. Taking pictures of the measured object from a larger distance or the use of appropriate digital tools (some of them are available in standard photo-editing soft-

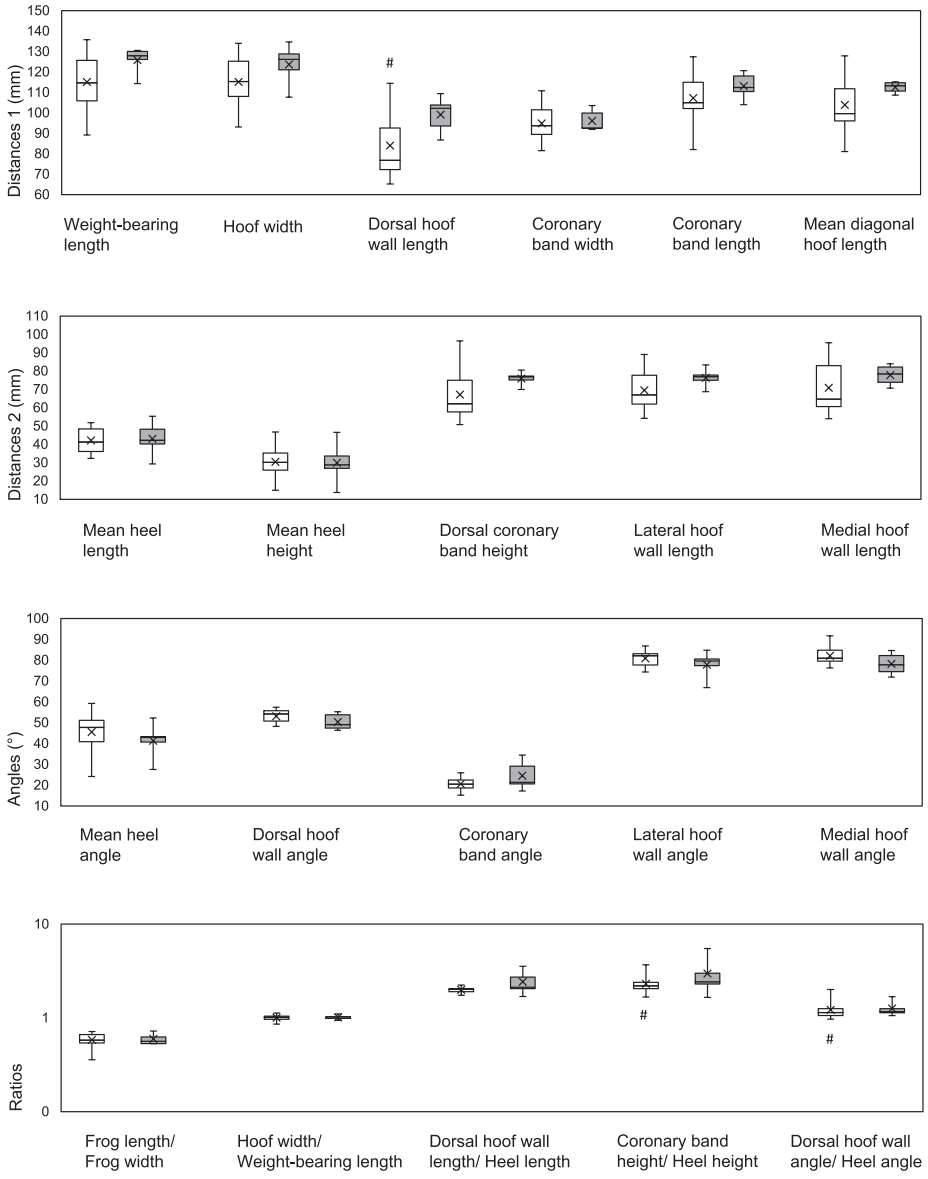

Fig. 7. Differences between measures of hooves without (white boxes, left side of the pairs) and with (grey boxes, right side) Long toes. No significant differences between affected and non-affected hooves. Boxes span the interquartile range of the measured values on the y-axis (n=16). The inside lines indicate the median and the × symbol mean values. Whiskers extend to the minimum and maximum values. Data sets that are not normally distributed are marked with a hash symbol. (For interpretation of the references to color in this figure legend, the reader is referred to the Web version of this article.)

ware based on the used objective) might be helpful to circumvent distortion problems when measuring structures in photographs. As in radiographs, the parallax effect can also lead to virtual distortion of the structures.

Three of the five measures showing no differences between the methods (Diagonal hoof length, Frog length and Frog width) could only be measured by four methods, excluding those which introduced the highest variability into our data set: CT and Radiography. Nonetheless, Lateral and Medial hoof wall length could be collected by more or less all methods (including Radiography and CT) without producing different results. Otherwise, the equivalency of the methods has to be rated for each single measure of interest.

Equivalency and differences between the methods detected in our study were not an artifact (e.g., due to small sample size). When comparing methods for measures that were taken from both lateral and medial hoof side (e.g., Lateral and Medial hoof wall length, Lateral and Medial diagonal hoof length, Lateral and Medial hoof width), nearly the same data distribution and differences between methods were detected.

4.2. Differences Between Measuring Methods for Individual Hoof Measures

The post-hoc analysis of our data provided a detailed overview of differences between the measuring methods for each individual measure (Supplement 2). A summary of differences including possible explanations are given in Table 3. Selected measures will be discussed in detail.

Measures that could be captured equally with all methods are Lateral and Medial hoof wall length. This differed surprisingly from the results for Dorsal hoof wall length, the reason for that not being entirely clear. The proximal and distal landmarks for these measures are similar, but their exact identification was even more complicated for Lateral and Medial hoof wall length, where

Table 3
Explanations for nonequivalence between hoof measuring methods for measures with confirmed differences between the methods (post-hoc Tukey's test, $P < .05$, cf. Supplement 2).

	Measure	Nonequivalent Measuring Methods	Possible Reasons for Nonequivalence Between Methods
Linear measures	Weight-bearing length	Radiography vs. all other methods (except CT) Microscribe vs. Direct measurements, Scaled photographs, Radiography	Radiography tends to overestimate: magnification due to conic beam and parallax effect, summation shadow might obscure palmar landmark Palmar landmark has to be constructed for Microscribe and Direct measurements
	Hoof width	Radiography vs. all other methods Microscribe vs. Photogrammetry, Radiography, CT Direct measurements vs. Photogrammetry, Radiography, CT CT vs. Direct measurements, Microscribe vs. Radiography	Radiography overestimates due to magnification and parallax effect (widest hoof part is half a hoof length away from detector). In general, definition of the widest hoof part is complicated for all methods; slightly oblique projection/ measuring might have a large effect
	Dorsal hoof wall length	Direct measurements vs. all other methods (except Scaled photographs) CT vs. all other methods (except Microscribe) Radiography vs. all other methods (except Scaled photographs) Scaled photographs vs. all other methods (except Radiography)	Nearly no equivalency between methods, suggests difficult definition of landmarks and/or projection or slice planes; uniform treatment of the problem of rounded or broken dorsal hoof wall tip is necessary
	Coronary band length	Radiography vs. all other methods Microscribe vs. all other methods except Direct measurements Direct measurements vs. Scaled photographs, Radiography and CT	Nearly no equivalency between methods. Difficult definition of landmarks – needs artificial markers in radiographs and shaved limbus in methods relying on external hoof appearance
	Coronary band width	No equivalences between methods except Direct measurements vs. Microscribe, CT	as Coronary band length, danger of oblique measuring/ projection, difficult definition of the widest hoof part
	Heel width	Microscribe vs. all other methods	The landmarks (from lateral to medial most palmar part of *Pars inflexa*) may not be defined precisely enough, fresh hoof trim enhances landmark visibility
	Dorsal coronary band height	Direct measurements vs. all other methods (except Scaled photographs) Radiographs vs. all other measures Scaled photographs vs. Photogrammetry, Radiography, CT	as Coronary band length
	Lateral hoof wall length	Scaled photographs vs. Direct measurements, Microscribe, Photogrammetry	Nearly all methods were equivalent (for Medial hoof wall length all methods were equivalent). Scaled photographs underestimate – oblique hoof wall on plane photograph
	Lateral and medial hoof width	Radiography vs. all other methods Microscribe vs. Direct measurements, Photogrammetry, Radiography, CT	Radiography overestimates, Lateral more than Medial hoof width. Magnification effect of conic beam (widest hoof part is half a hoof length away from detector). Other differences between methods very small.
	Lateral and Medial heel length	CT vs. all other methods	Challenging definition of the section plane for reconstruction of CT slices – sagittal plane does not show complete heel if it is slightly oblique: underestimation. Proximal landmark (boundary between coronary band and horn wall) moves virtually when changing the viewing settings, standard soft window setting may have shown the border too far distally
	Bulb distance	Photogrammetry vs. all other methods Scaled photographs vs. all other methods	Photogrammetry and Scaled photographs underestimate – resolution of photogrammetry models too small for clear landmark definition, Scale in the photos at level of *Margo solearis* instead of heel
	Lateral and Medial heel height	CT vs. all other methods Photogrammetry vs. all other methods	Proximal landmark (boundary between coronary band and horn wall) moves virtually when changing the CT viewing settings, standard soft window setting may have shown the border too far distally. Photogrammetry: proximal end of palmar coronary band covered with hair, identification difficult even after shaving
Angular measures	Lateral and Medial hoof wall angle	nearly all comparisons with significant differences (except Microscribe vs. CT and Direct measurements vs. Radiography)	Exact position of the landmark at the widest point of the hoof was challenging for the following methods: Microscribe, Direct measurements, Photogrammetry and CT. For Radiography and Scaled photographs: possible problem of oblique projection
	Dorsal hoof wall angle	Scaled photographs vs. all other methods (except CT) CT vs. all other methods (except Scaled photographs) Microscribe vs. Radiography	Scaled photographs underestimate– distortion by camera lenses CT underestimates – difficult definition of slice planes
	Lateral and Medial proximal hoof wall angle	Scaled photographs vs. all other methods	Lens distortion and projection artefacts
	Coronary band angle	Microscribe vs. Direct measurements and Photogrammetry Direct measurement vs. Radiography	Generally good equivalence – well defined and easy to measure. Microscribe produced outliers that might have resulted in detection of differences
	Lateral and Medial heel angle	Scaled photographs vs. all other methods Direct measurements vs. photogrammetry	Scaled photographs overestimate. Inferior resolution of lateral and medial heel due to their dark colour and projection over each other in lateral photographs
	Mediolateral symmetry	Microscribe vs. all other methods	Microscribe (and Photogrammetry) are based on coronary band position, Radiography and CT on distal interphalangeal joint

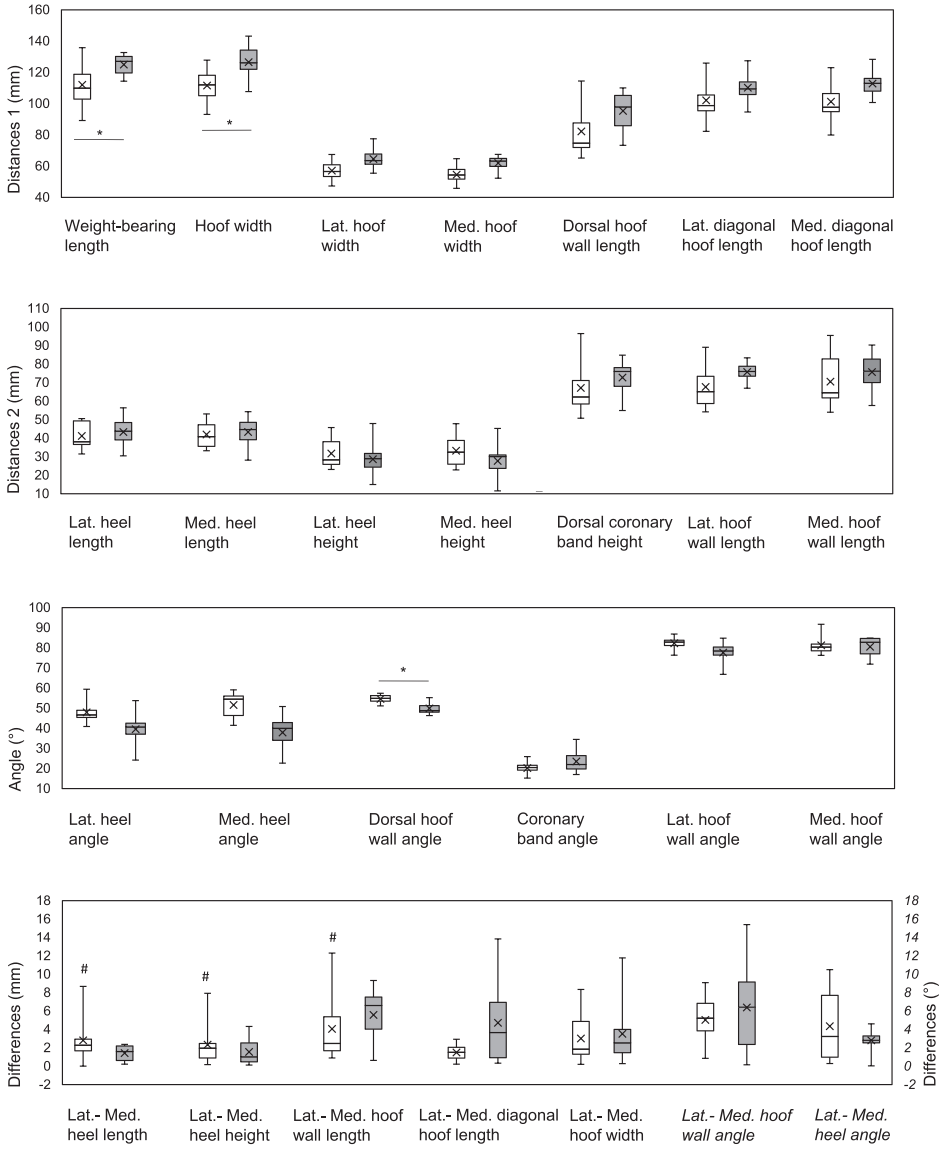

Fig. 8. Differences between measures of samples without (white boxes, left side of the pairs) and with (grey boxes, right side) the conformation "Diagonal hoof". Significant differences between Diagonal hooves and all other hooves were detected for two linear measures and one angle (asterisks, post-hoc univariate ANOVA, $P < .05$). Boxes span the interquartile range of the measured values on the y-axis (n=16). The inside lines indicate the median and the × symbol mean values. Whiskers extend to the minimum and maximum values. Groups that are not normally distributed are marked with a hash symbol. Lat. = lateral, med. = medial. (For interpretation of the references to color in this figure legend, the reader is referred to the Web version of this article.)

the "widest point" of the hoof had to be found. Differences between Photogrammetry and the other methods can be explained by the fact that the measuring tool did not allow to define the distal reference point "on the ground" in extension of the hoof wall, when its *Margo solearis* was broken or rounded [7,52]. However, this applies equally to Dorsal, Lateral and Medial hoof wall length.

Some further discrepancies might be caused by the fact that the individual methods measure different structures. A prominent example is the Weight-bearing length. In radiographs and scaled photographs, the complete hoof length touching the ground could be easily determined. In contrast, the CT images used for this purpose would be the axial sections defined by toe tip and central groove of the frog. The Weight-bearing length that could be measured in this slice was smaller, since the heels of the hoof with their weight-bearing margin extend further in palmar/plantar direction than the frog.

The absence of significant differences between the individual methods for Frog width despite a significant ANOVA is an interesting occurrence. Simulations have shown that the more conservative post-hoc tests may fail to recognize differences between individual data sets, while the omnibus test is still significant [53]. In our case, this effect might be ascribed to a combination of a rather weak global effect (ANOVA $P = .029$) and a small sample size.

4.3. MicroScribe as a Tool for Collecting Hoof Measurements

The MicroScribe tool is increasingly used for different morphometric tasks [24–28] but has not yet been tested comprehensively for capturing the hoof shape [29]. In our study, the Microscribe values for linear measures showed good equivalency with methods based on real hooves (Photogrammetry, Scaled photographs, Direct measurements), even if landmarks such as hoof midline, widest part of the hoof etc., were located by eyeballing them. Our

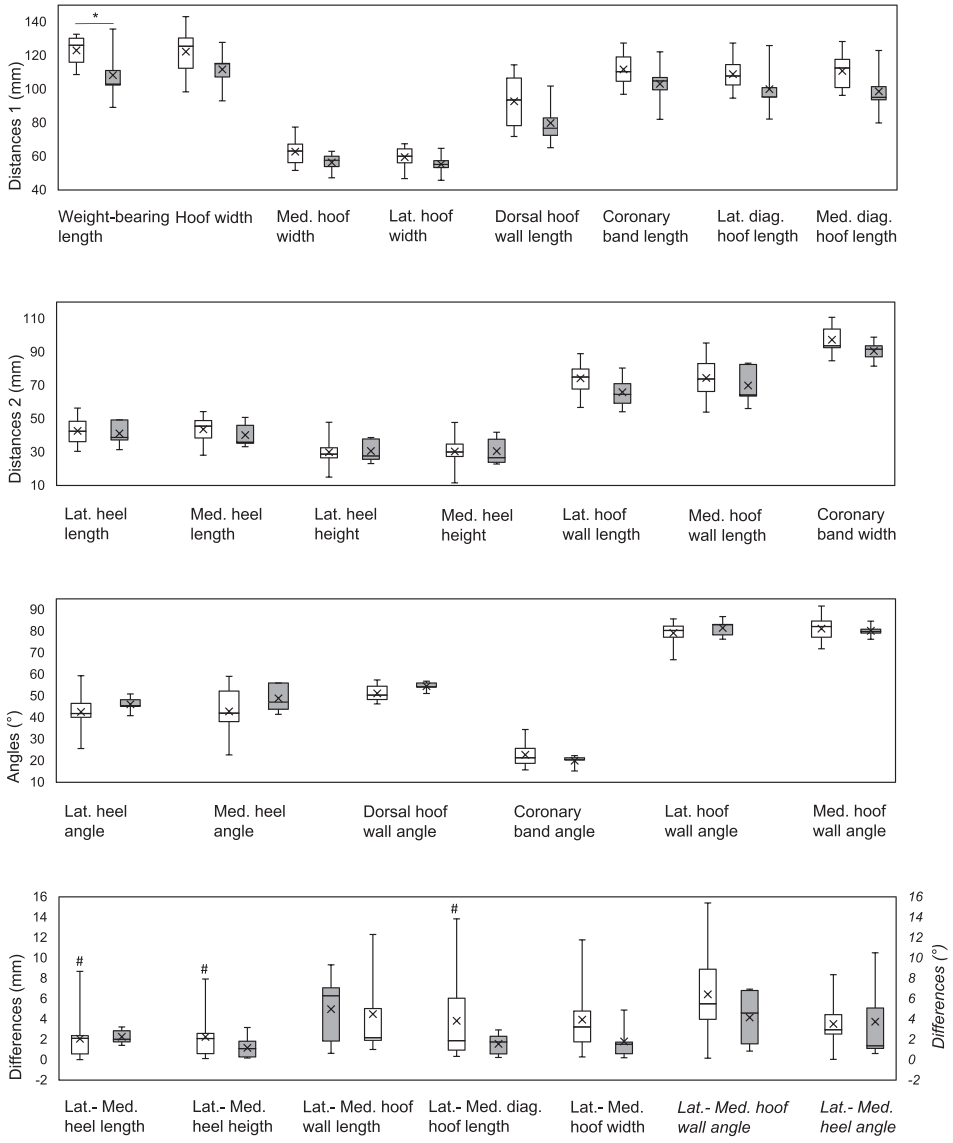

Fig. 9. Differences between measures of asymmetric (white boxes, left side of the pairs) and symmetric (grey boxes, right side of the pairs) hooves. Significant differences between the conformations could only be detected for Weight-bearing length (asterisk, post-hoc univariate ANOVA, $P < .05$). Boxes span the interquartile range of the measured values on the y-axis (n=16). The inside lines indicate the median and the × symbol mean values. Whiskers extend to the minimum and maximum values. Groups that are not normally distributed are marked with a hash symbol. Lat. = lateral, med. = medial, diag. = diagonal. (For interpretation of the references to color in this figure legend, the reader is referred to the Web version of this article.)

pilot study revealed small intra- and interobserver variability for Microscribe measurements (not shown). However, the tool seems to be less suitable for collecting angular measurements in hooves, as demonstrated by comparison with other methods (Fig. 5, Supplement 3). One has to be aware that the uneven surface of the equine hoof may contribute considerably to the large differences. If the small conical MicroScribe probe used in our study slid over irregularities of the hoof capsule while recording the respective landmark, it had a large impact on the measured angles as discussed above. The use of probes with a larger contact surface might be helpful to prevent this problem. Barmou et al. [54] reported similar challenges as in our study when comparing Radiography and Microscribe for human cephalometry, where four of the seven analyzed angles were not equivalent between methods, although low inter- and intra-observer variability was detected for Microscribe angular measurements by these and other authors [55,56]. Linear measurements, in contrast, are less affected.

The Mediolateral symmetry angle, whose Microscribe value differed considerably from that of the other methods, represented a special case in our study. This measure is mostly based on the position of the distal interphalangeal joint in relation to the ground and thus recorded from radiographs, CT slices or physical slices of the hoof [57,58]. Microscribe, but also Photogrammetry, rely instead on the relative position of the coronary band to the ground, providing informative data but not the same as bone landmarks. Interestingly, Photogrammetry data clustered with CT and Radiography values in our samples, not with Microscribe as expected. This might be a combined effect of probe positioning difficulties as described above and the fact that Photogrammetry, in general, is less suitable for angle measuring. In general, Mediolateral symmetry has been measured based on many different landmarks, for example the *Margo solearis* of *Phalanx distalis* [57,59,60], *Foramen soleare laterale* and *mediale* of *Phalanx distalis* [60,61], distal interphalangeal joint space [62] and Lateral and Medial heel length

[35]. Thus, results for this measure often cannot be compared between publications.

4.4. Hoof Conformation

Subjective assessment of the limb conformation (including hooves) is a part of the orthopedic examination [62]. To objectify this approach, endeavors have been made to describe hoof conformations based on certain measurements or their relation to each other. Examples are Long toes and Under-run heels [34].

It can be hypothesized that additionally to the measures defining the hoof shape of interest, for example, toe angle $< 45°$ or $< 50°$ (details differ between publications) for forehooves defining "Long toes"; [34,63,64], other measures and relations are affected, too. For the hooves analyzed for our study, this was at least partially confirmed.

4.4.1. Under-Run Heels

Hooves with Under-run heels are defined by heel angles that are at least 5° lower than the Dorsal hoof wall angle [65]. In our samples, the difference between the two angles was indeed larger in hooves with Under-run heels, however, this difference was not significant (mean 10.63 ° vs. mean 4.61° $P = .086$; cf. Fig. 6). In the same way, the ratio Dorsal hoof wall angle/ Heel angle was expected to differ significantly with higher values in the affected hooves but failed to do so.

Hooves with Under-run heels also showed lower Diagonal hoof length, Heel length, Heel height and Lateral and Medial hoof wall length, as well as a higher ratio between Hoof width and Weight-bearing length. Some of these differences result from the changed hoof geometry: With a smaller Heel angle, the proximal landmark of Mean heel height gets closer to the ground, reducing measured values. The Mean diagonal hoof length was reduced due to the dorsal displacement of the palmar landmark in Under-run heels (cf. Table 1).

In normal hooves, the ratio Hoof width/ Weight-bearing length should be around 1 or slightly larger [1, and Jackson 1992, cited by 34]. In our samples this ratio was significantly larger in hooves with Under-run heels as expected. This seems to be mainly a result of the relative shortening of the *Facies contactus* of *Facies solearis* in the affected hooves.

Interestingly, there was also a set of measures with significant differences between hooves without and with Under-run heels, which we did not expect. The Heel length was smaller in affected hooves instead of being larger as expected. Since the Microscribe method is based on setting landmarks in the real three dimensional space, perspective foreshortening is no explanation. However, landmark definition at the boundary between the heel and *Facies contactus* was not easy in hooves with Under-run heels. Similarly, an explanation as to why Lateral and Medial hoof wall length was smaller in hooves with under-run heels is not trivial. It might be a result of the pronounced palmar sloping of the coronary band in these hooves.

4.4.2. Long Toe

Forehooves with Long toe have Dorsal hoof wall angles smaller than 50° [63] or even smaller than 45° [64]. In our study, the Dorsal hoof wall angle was smaller in the long toes group but did not differ significantly from that in all other hooves. In fact, none of the samples had angles smaller than 45°, and only in five specimens the dorsal hoof wall angle was smaller than 50°, three of which were classified as Long toe (see Supplement 1).

In addition, we would have expected the Dorsal coronary band height, the Coronary band angle and the Heel angle to be smaller in the group of affected hooves. For Dorsal coronary band height and Coronary band angle, this was not the case. On the contrary, the measures were slightly higher in the group of hooves with long toes. Only the Heel angle seems to discriminate between the conformations but did not prove to differ significantly.

The lack of significant differences between hooves with and without Long toe in our sample might be explained by the low number of Long toe cases. We have also filed hooves in the long toe group that only "tended to long toe" by expert diagnosis, which increased the number of cases but not the likelihood of a significant result.

4.4.3. Diagonal Hoof

A diagonal hoof has similar angles in diagonally opposite wall sections, for example, with a steep palmarolateral hoof wall, the diagonal dorsomedial half is also steep, while the contralateral hoof wall parts are flatter [64]. Its *Facies solearis* has a typical shape: two curved and two rather flat segments of the weight-bearing margin face each other in diagonal direction [66]. It is extraordinarily difficult to describe this hoof shape using the standard measures taken from strictly dorsal, lateral/medial and palmar/plantar reference points. In an "ideally diagonal" hoof, these sites would be the transition points between long, flared and short, steep hoof wall segments and thus not differ much from "normal". Certain pointers towards diagonal hoof shape might be provided by the differences of Medial and Lateral hoof wall length, diagonal hoof length, hoof wall angle and hoof width, but none of them detected significant differences between Diagonal and nondiagonal hooves in our samples.

The Diagonal hooves of our study were somewhat larger, as can be seen from Weight-bearing length and Hoof width, both differing significantly between diagonal and nondiagonal hooves, but also most of the other linear measures. Possibly, the hooves classified as diagonal have not been trimmed recently.

4.4.4. Symmetric Hoof

The Symmetric forehoof is regular and even but might have a slightly steeper medial hoof wall angle [64]. For the samples classified as Symmetric hooves in our study, we therefore expected small differences between the lateral/medial measures in contrast to larger differences for asymmetric hooves. This was not the case. All differences between lateral and medial distances and angles were small and did not differ between the conformations, with the possible exception of Lateral – Medial hoof width. This was an interesting finding, even if our sample size was not very large. The distinction between hoof (a)symmetry (hoof balance) on one side and differences between medial and lateral hoof (wall) measures on the other side is discussed quite hotly by farriers (e.g., more than 1000 entries for the search term "hoof balance" at https://www.americanfarriers.com/, accessed July 29, 2022). They point out that for example, Medial and Lateral hoof wall length may well be the same, but the hoof itself is still asymmetric and needs to be treated as such. Shape of the coronary band, axis of the whole limb or measuring the pressure exerted on the ground at different points of the *Facies contactus* seem to be better indicators for hoof asymmetry than mere differences between lateral and medial hoof measures [67,68].

As for the Diagonal hoof, asymmetric hooves tended to be somewhat larger than Symmetric hooves. This difference was most pronounced for measures of the dorsal part of the hoof and even significant for the Weight-bearing length. Smaller hooves thus might be generally more symmetric, or Symmetric hooves were freshly trimmed. For our sample set, the latter seems to be true, since heel angles and dorsal hoof wall angle were slightly larger in symmetrical hooves, which is a usual result of trimming.

Table 4
Overview of recommendations for the use of six measuring methods for hoof biometry.

Method	Notes and Recommendations
Direct measurements	• cheap, quick and easy • applicable in conscious live horses • provides very consistent results • usually, a limited number of single measures is taken • precision smaller than for advanced digital measuring tools (Radiography, CT) • measuring of inner structures (e.g., bones) only in physical sections of cadaver material • some angle measures cannot be taken (very small angles, angles where correct positioning of the protractor is not possible or possible only after physical sectioning of the hoof) • limited possibility to define virtual, "free-floating" reference points (e.g., in prolongation of the hoof wall to the ground line, when the wall is broken or rounded)
Scaled photographs	• cheap • mcecessary • precision dependent on measuring device (ruler vs. digital tools) • measuring of inner structures (e.g., bones) only in physical sections of cadaver material • limited applicability in conscious live horses • use telephoto lens/zooming in to prevent bevel distortion of photographs; for precise measuring, computational lens distortion correction is inevitable • less suitable for angle measurements, at least without distortion correction
Microscribe	• a large number of data points in 3D space can be collected in a very short time • data point vectors available directly without prior reconstruction – facilitates advanced modelling • virtually no costs if the MicroScribe tool is available • measures have to be calculated; free software for a standard set of hoof measurements available via zenodo.org • precision dependent on reference point definition, use of appropriate probe tips (not too fine, since hoof surface is not smooth) is recommended • limited applicability in live horses • measuring of inner structures (e.g., bones) only in physical sections of cadaver material
Photogrammetry	• cheap when basic free photogrammetry software and measuring tools are used • creates nearly photorealistic 3D reconstructions that can be used for repeated measuring or other purposes • might require additional preparatory steps to ensure reference point visibility • not applicable for inner hoof structures (for physical sections, scaled photographs or scans are easier and quicker to prepare) • limited applicability in conscious live horses • no possibility to define virtual, "free-floating" reference points, at least in the basic free software
Radiography	• cheapest nondestructive method to measure outer as well as inner hoof structures • applicable in conscious live horses • easily included in standard clinical examination • projection image – easy definition of maximal widths and lengths of structures • high precision of the measuring tools in digital image viewers • measurements can be easily documented and repeated if necessary • use radio-opaque markers for definition of soft tissue reference points • for generation of accurate ("real") measures, correction of projection magnification and parallax distortion is necessary, otherwise radiography overestimates
CT	• nondestructive method to measure outer as well as inner hoof structures • regarded as method of choice for measuring bony structures • measurements can be easily documented and repeated if necessary • high precision of the measuring tools in digital image viewers • can be used to generate 3D reconstructions of outer and inner hoof structures; measurements in rendered models is possible if required • pricy • not applicable in conscious live horses • finding soft tissue reference points is difficult • definition of slice levels and reference points requires more training and experience than other methods; danger of faulty measuring results when using incorrect slice levels

4.5. Limitations of the Study

For interpretation of the homogeneity of measurement results it is necessary to take into account that the 16 hooves included in the current study did not originate from a homogeneous group of horses. Therefore, a certain spread of data was to be expected. Still, at least for linear measurements, the range of values was quite homogeneous with the different measuring methods, suggesting that the precision of all employed techniques was comparable. Angular dimensions, however, should not be dependent on the hoof size. The data spread depicted in Fig. 3 can probably be ascribed to the variability of hoof shape, but also to imprecisions in landmark positioning as described above.

For the purpose of this study, we have regarded nonsignificant differences between the methods as an indicator for method equivalency. From a statistical point of view, this approach is not entirely correct, since the null hypothesis for comparisons of means is "no differences between groups". This is afterwards rejected in case that the appropriate tests (one-way repeated measures ANOVA and its post hoc tests) show significant differences. If no significant differences are detected, groups (in our case measuring methods) can still differ from each other, but with a probability of 95%, these differences are random. However, since the box plots in Fig. 2 show homogeneous results for measures with nonsignificant differences, the according methods might be regarded as equivalent.

Due to the small number of hooves with the individual conformations of interest, the one-way MANOVA testing was split into several sub-tests in order to meet the assumption that there have to be more cases in each group than the number of dependent variables. This partly revokes the main benefit of MANOVA – the reduction of likelihood of alpha error accumulation. We still decided to use this approach in order to identify possible measures that are able to discriminate between the most frequent hoof conformations but are less obvious than the conformation-defining lengths, angles, ratios and differences described in literature. A larger sample size would help to overcome this problem. Furthermore, MANOVA testing is discouraged with highly positively correlated variables. This assumption was not met entirely by our data set. It was dealt with as described in Material and methods (see paragraph 2.4). The lack of normal distribution in some of the data sets (cf. Figs. 6–9) was disregarded when performing the one-way MANOVA, as this test is considered robust to violation of this assumption [38].

5. Conclusions

Hoof measures collected using different methods cannot be regarded automatically as equivalent without prior testing. In frame of one study, one measure should be collected using only one method. In some cases, different methods measure different structures. Examples are Weight-bearing length (methods based on virtual sections vs. methods based on projection images or whole hooves) or Mediolateral symmetry (landmarks based on articular surface vs. landmarks based on coronary band). In these cases, the methods should be chosen based on the biological question. An overview of recommendations for the use of the individual measuring methods is given in Table 4.

Measures based on clear landmarks (e.g., Lateral and Medial diagonal hoof length, Frog length), will mostly produce similar results irrespective of the method.

Radiography tends to overestimate distances due to magnification and parallax effect. Mathematical correction may be considered if necessary. Photogrammetry and Scaled photographs are less suitable for measuring hoof angles. Other methods such as CT and Radiography or even Direct measurements provide more consistent results.

The precision of the tested measurement methods is comparable as could be shown by the similar data spread for all methods in each individual measure (Figs. 2 and 3).

The MicroScribe tool can readily be used for collection of hoof measurements. The values for linear measures showed good equivalency with other methods based on real hooves (Photogrammetry, Scaled photographs, Direct measurements). For angular measurements, the unevenness of the hoof surface has to be taken into account, an appropriate probe has to be chosen. The recording of landmarks with the MicroScribe tool is quick and needs only a computer or equivalent digital device, no other accessories. If only few landmarks are recorded, it might be even attempted in live animals (in the loaded limb to prevent movement between landmark recording). No intermediate reconstruction step is necessary, length and angles are calculated directly from the vectors. Compared with Direct measurements, length measurements with the MicroScribe tool are not impeded by deformities of the hoof wall, which may render applying rulers and other measuring tools difficult.

Even if hoof shapes can be classified based on different measurements and their relations or differences, diagnosis by a skilled veterinarian should still be included in such studies, since not all hoof conformations can be detected based on a number of standard measures.

Acknowledgments

We would like to thank Dr. Katrin Schieder for her great help and expertise in the creation of the radiographs. Furthermore, a big thank you goes to Bibiane Pollak for the generation of the CT data sets.

Financial Disclosure

This work was supported by the Hochschuljubiläumsfonds of City Vienna [H-291437/2019].

Supplementary materials

Supplementary material associated with this article can be found, in the online version, at doi:10.1016/j.jevs.2022.104195.

References

[1] Kane AJ, Stover SM, Gardner IA, Bock KB, Case JT, Johnson BJ, et al. Hoof size, shape, and balance as possible risk factors for catastrophic musculoskeletal injury of thoroughbred racehorses. Am J Vet Res 1998;59:1545–52 ISSN:0029645.
[2] Bellenzani MCR, Merritt JS, Clarke S, Davies HMS. Investigation of forelimb hoof wall strains and hoof shape in unshod horses exercised on a treadmill at various speeds and gaits. Am J Vet Res 2012;73:1735–41. doi:10.2460/ajvr.73.11.1735.
[3] Souza AF, Kunz JR, Laus R, Moreira MA, Muller TR, Fonteque JH. Biometrics of hoof balance in equids. Arq Bras Med Vet Zoo 2016;68:825–31. doi:10.1590/1678-4162-8848.
[4] Hinterhofer C, Weißbacher N, Bucher HHF, Peham C, Stanek C. Motion analysis of hoof wall, sole and frog under cyclic load in vitro: deformation of the equine hoof shod with regular horse shoe, straight bar shoe and bare hoof. Pferdeheilkunde 2006;22:314–19. doi:10.21836/PEM20060311.
[5] Pares i Casanova PM, Oosterlinck M. Hoof size and symmetry in young Catalan Pyrenean horses reared under semi-extensive conditions. J Equine Vet Sci 2012;32:231–4. doi:10.1016/j.jevs.2011.08.020.
[6] Hagen J, Kojah K, Geiger M. Correlations between the equine metacarpophalangeal joint angulation and toe conformation in statics. Open Vet J 2018;8:96–103. doi:10.4314/ovj.v8i1.15.
[7] Hampson BA, de Laat MA, Mills PC, Pollitt CC. The feral horse foot. Part A: observational study of the effect of environment on the morphometrics of the feet of 100 Australian feral horses. Aust Vet J 2013;91:14–22. doi:10.1111/avj.12017.
[8] Faramarzi B, Hung F, Fanglong D. Correlational characteristics of hoof conformation and midstance kinetics at walk. J Equine Vet Sci 2020;94:1–6. doi:10.1016/j.jevs.2020.103208.
[9] Pezzanite L, Bass L, Kawcak C, Goodrich L, Moorman V. The relationship between sagittal hoof conformation and hindlimb lameness in the horse. Equine Vet J 2019;51:464–9. doi:10.1111/evj.13050.
[10] Decurnex V, Anderson GA, Davies HMS. Influence of different exercise regimes on the proximal hoof circumference in young Thoroughbred horses. Equine Vet J 2009;41:233–6. doi:10.2746/042516409X393220.
[11] Hampson BA, Ramsey G, Macintosh AMH, Mills PC, de Laat MA, Pollitt CC. Morphometry and abnormalities of the feet of Kaimanawa feral horses in New Zealand. Aust Vet J 2010;88:124–31. doi:10.1111/j.1751-0813.2010.00554.x.
[12] Dyson SJ, Tranquille CA, SN Collins, Parkin TDH, Murray RC. External characteristics of the lateral aspect of the hoof differ between non-lame and lame horses. Vet J 2011;190:364–71. doi:10.1016/j.tvjl.2010.11.015.
[13] Cruz CD, Thomason JJ, Faramarzi B, Bignell WW, Sears W, Dobson H, Konyer NB. Changes in shape of the Standardbred distal phalanx and hoof capsule in response to exercise. Equine Comp Exerc Physiol 2006;3:199–208. doi:10.1017/S1478061506617258.
[14] Goulet C, Olive J, Rossier Y, Beauchamp G. Radiographic and anatomic characteristics of dorsal hoof wall layers in nonlaminitic horses. Vet Radiol Ultrasound 2015;56:589–94. doi:10.1111/vru.12280.
[15] Eliashar E, McGuigan MP, Wilson AM. Relationship of foot conformation and force applied to the navicular bone of sound horses at the trot. Equine Vet J 2004;36:431–5. doi:10.2746/0425164044868378.
[16] Thieme K, Ehrle A, Lischer C. Radiographic measurements of the hooves of normal ponies. Vet J 2015;206:332–7. doi:10.1016/j.tvjl.2015.10.005.
[17] Cripps PJ, Eustace RA. Radiological measurements from the feet of normal horses with relevance to laminitis. Equine Vet J 1999;31:427–32. doi:10.1111/j.2042-3306.1999.tb03844.x.
[18] Kummer M, Lischer C, Ohlert S, Vargas J, Auer J. Evaluation of a standardised radiographic technique of the equine hoof. Schweiz Arch Tierheilk 2004;146:507–14. doi:10.1024/0036-7281.146.11.507.
[19] Labens R, Redding WR, Desai KK, vom Orde K, Mansmann RA, Blikslager AT. Validation of a photogrammetric technique for computing equine hoof volume. Vet J 2013;197:625–30. doi:10.1016/j.tvjl.2013.04.005.

[20] Jordan P, Willneff J, DÁpuzzo N, Weißhaupt M, Wistner T, Auer J. Photogrammetric measurement of deformations of horse hoof horn capsules. Proc SPIE 2001;4309:204–11. doi:10.1117/12.410886.
[21] Grundmann INM, Drost WT, Zekas LJ, Belknap JK, Garabed RB, Weisbrode SE, et al. Quantitative assessment of the equine hoof using digital radiography and magnetic resonance imaging. Equine Vet J 2015;47:542–7. doi:10.1111/evj.12340.
[22] de Zani D, Polidori C, di Giancamillo M, Zani DD. Correlation of radiographic measurements of structures of the equine foot with lesions detected on magnetic resonance imaging. Equine Vet J 2016;48:165–71. doi:10.1111/evj.12411.
[23] Bolt D, Carrier ME, Sheridan KS, Manso-Diaz G, Berner D. Measurement accuracy of foot conformation parameters on low-field magnetic resonance images in horses. J Equine Vet Sci 2022;112:1–8. doi:10.1016/j.jevs.2022.103894.
[24] Nicholson E, Harvati K. Quantitative analysis of human mandibular shape using three-dimensional geometric morphometrics. Am J Phys Anthropol 2006;131:368–83. doi:10.1002/ajpa.20425.
[25] Masharawi Y, Dar G, Peleg S, Steinberg N, Dvora AN, Salame K, et al. Lumbar facet anatomy changes in spondylolysis: a comparative skeletal study. Eur Spine J 2007;16:993–9. doi:10.1007/s00586-007-0328-8.
[26] Masharawi Y, Salame K, Mirovsky Y, Peleg S, Dar G, Steinberg N, et al. Vertebral body shape variation in the thoracic and lumbar spine: Characterization of its asymmetry and wedging. Clin Anat 2008;21:46–54. doi:10.1002/ca.20532.
[27] McDowell JL, LÁbbe EN, Kenyhercz MW. Nasal aperture shape evaluation between black and white South Africans. Forensic Sci Int 2012;222 397.e1-397.e6. doi:10.1016/j.forsciint.2012.06.007.
[28] Dietrich J, Handschuh S, Steidl R, Böhler A, Forstenpointner G, Egerbacher M, et al. Muscle fibre architecture of thoracic and lumbar longissimus dorsi Muscle in the horse. Animals 2021;11:915. doi:10.3390/ani11030915.
[29] Hanley J. Elastomeric hoof boots. Masters dissertation. Dublin Institute of Technology 2003. doi:10.21427/D7NG7K.
[30] Sellke, L. Surface coordinates of 16 equine hooves generated by the MicroScribe® tool (data set) 2022. Version 1.0. Institute of Morphology, Workgroup Anatomy. doi:10.5281/zenodo.7028334.
[31] Sellke L, Patan-Zugaj B, Witter K. Nomenclature of equine hoof measurements – a systematic literature review. Pferdeheilkunde 2020;36:238–51 doi:10.21836/PEM20200306.
[32] Labuschagne W, Rogers CW, Gee EK, Bolwell CF. A cross-sectional survey of forelimb hoof conformation and the prevalence of flat feet in a cohort of thoroughbred racehorses in New Zealand. J Equine Vet Sci 2017;51:1–7. doi:10.1016/j.jevs.2016.11.013.
[33] Holroyd K, Dixon JJ, Mair T, Bolas N, Bolt M, David F, Weller R. Variation in foot conformation in lame horses with different foot lesions. Vet J 2013;195:361–5. doi:10.1016/j.tvjl.2012.07.012.
[34] Parks AH. Foot balance, conformation, and lameness. In: Ross M, Dyson SJ, editors. Lameness in the Horse. Missouri: Elsevier Saunders; 2011. p. 282–303.
[35] Moyer WA, Carter GK. Diagnostic evaluation of the equine foot. In: Floyd AE, Mansmann RA, editors. Equine Podiatry. Missouri: Elsevier Saunders; 2007. p. 112–27.
[36] Cimrman, R. Hoof MicroScribe data statistics- software to generate measurements out of surface coordinates of the equine hoof (data set). New Technologies Research Centre Pilsen. doi:0.5281/zenodo.6962789.
[37] Bader M. MB-ruler, MB-Softwaresolutions 2019; 15 Jul 2019. http://www.markus-bader.de/MB-Ruler/index.d.php.
[38] Finch H. Comparison of the performance of nonparametric and parametric MANOVA test statistics when assumptions are violated. Methodology 2006;1:27–38. doi:10.1027/1614-1881.1.1.27.
[39] Dyson SJ, Tranquille CA, SN Collins, Parkin TDH, Murray RC. An investigation of the relationships between angles and shapes of the hoof capsule and the distal phalanx. Equine Vet J 2011;43:295–301. doi:10.1111/j.2042-3306.2010.00162.x.
[40] Faramarzi B, McMicking H, Halland S, Kaneps A, Dobson H. Incidence of palmar process fractures of the distal phalanx and association with front hoof conformation in foals. Equine Vet J 2015;47:675–9. doi:10.1111/evj.12375.
[41] Shahkhosravi NA, Son J, Davies HMS, Komeili A. An investigation into different measurement techniques to assess equine proximal hoof circumference. J Equine Vet Sci 2022;115:104028. doi:10.1016/j.jevs.2022.104028.
[42] Stevens PM. Radiographic distortion of bones: a marker study. Orthoped 1989;12:1457–63. doi:10.3928/0147-7447-19891101-11.
[43] Nilsson T, Ahlqvist J, Johansson M, Isberg A. Virtual reality for simulation of radiographic projections: validation of projection geometry. Dentomaxillofac Radiol 2004;33:44–50. doi:10.1259/dmfr/22722586.
[44] Kumar V, Ludlow JB, Mol A, Cevidanes L. Comparison of conventional and cone beam CT synthesized cephalograms. Dentomaxillofac Radiol 2007;36:249–310. doi:10.1259/dmfr/98032356.
[45] Goldman AH, Hoover KB. Source-to-detector distance and beam center do not affect radiographic measurements of acetabular morphology. Skeletal Radiol 2017;46:477–81. doi:10.1007/s00256-017-2571-3.
[46] Chan EF, Cockman MD, Goel P, Newman PS, Hipp JA. Characterization of the mid-coronal plane method for measurement of radiographic change in knee joint space width across different levels of image parallax. Osteoarthritis Cartilage 2021;29:1306–13. doi:10.1016/j.joca.2021.06.006.
[47] Wells TR, Landing BH, Padua EM. The question of parallax-effect on radiographic assessment of short trachea in infants and children. Pediatr Radiol 1991;21:490–3. doi:10.1007/BF02011719.
[48] Foster GP, Dunn AK, Abraham S, Ahmadi N, Sarraf G. Accurate measurement of mitral annular dimensions by echocardiography: Importance of correctly aligned imaging planes and anatomic landmarks. J Am Soc Echocardiography 2009;22:458–63. doi:10.1016/j.echo.2009.02.008.
[49] Sun C, Guo X, Wang P, Zhang B. Computational optical distortion correction based on local polynomial by inverse model. Opt 2017;132:388–400. doi:10.1016/j.ijleo.2016.12.069.
[50] Kim TH. An efficient barrel distortion correction processor for Bayer pattern images. IEEE Access 2018;6:28239–48. doi:10.1109/ACCESS.2018.2841013.
[51] Weng J, Zhou W, Ma S, Qi P, Zhong J. Model-free lens distortion correction based on phase analysis of fringe-patterns. Sensors 2021;21:209. doi:10.3390/s21010209.
[52] Clayton HM, Gray S, Kaiser LJ, Bowker RM. Effects of barefoot trimming on hoof morphology. Aust Vet J 2011;89:305–11. doi:10.1111/j.1751-0813.2011.00806.x.
[53] Chen T, Xu M, Tu J, Wang H, Niu X. Relationship between omnibus and post-hoc tests: an investigation of performance of the F test in ANOVA. Shanghai Arch Psychiatry 2018;30:60–4. doi:10.11919/j.issn.1002-0829.218014.
[54] Barmou MM, Hussain SF, Abu Hassan MI. Fiabilité et validité du système MicroScribe-3DXL par rapport au système céphalométrique radiographique: mesures angulaires. Int Orthodontics 2018;16:314–27. doi:10.1016/j.ortho.2018.03.006.
[55] Alobaidy MA, Soames RW. Evaluation of the coracoid and coracoacromial arch geometry on Thiel-embalmed cadavers using the three-dimensional MicroScribe digitizer. J Shoulder Elbow Surg 2016;251:136–41. doi:10.1016/j.jse.2015.08.036.
[56] Owaydhah WH, Alobaidy MA, Alraddadi AS, Soames RW. Three-dimensional analysis of the proximal humeral and glenoid geometry using MicroScribe 3D digitizer. Surg Radiol Anat 2017;39:767–72. doi:10.1007/s00276-016-1782-y.
[57] Bhatnagar AS, Pleasant RS, Dascanio JJ, Lewis SR, Grey A, Schroeder OE, Doyle K, Hall J, Splan RK. Hoof conformation and palmar process fractures of the distal phalanx in warmblood foals. J Equine Vet Sci 2010;30:349–55. doi:10.1016/j.jevs.2010.05.004.
[58] Sherlock C, Parks A. Radiographic and radiological assessment of laminitis. Equine Vet Educ 2013;25:524–35. doi:10.1111/eve.12065.
[59] Hagen J, Hüppler M, Häfner FS, Geiger MS, Mäder D. Untersuchung des Einflusses unterschiedlicher Bodenbeschaffenheiten auf die Ausrichtung der distalen Zehenknochen des Pferdes. Pferdeheilkunde 2015;31:578–86. doi:10.21836/PEM20150605.
[60] Hertsch B, Teschner D. Das Hornwachstum bei der chronischen Hufrehe des Pferdes. Tierarztl Prax 2011;39:163–70. doi:10.1055/s-0038-1624632.
[61] Reilly PT. In-shoe force measurements and hoof balance. J Equine Vet Sci 2010;30:475–8. doi:10.1016/j.jevs.2010.07.013.
[62] Baxter GM, Stashak TS. Examination for lameness. In: Baxter GM, editor. Adams & Stashaks lameness in horses. West Sussex: Wiley-Blackwell; 2011. p. 67–122.
[63] Turner TA. Examination of the equine foot. Vet Clin North Am Equine Pract 2003;19:309–32. doi:10.1016/S0749-0739(03)00023-3.
[64] Von Zadow C. Hufformen. In: Litzke LF, Rau B, editors. Der Huf. Stuttgart: Enke Verlag in MVS Medizinverlage, GmbH & Co KG; 2012. p. 114–19.
[65] Turner TA. Shoeing principles for the management of navicular disease in horses. J Am Vet Med Assoc 1986;189:298–301 ISSN:00031488.
[66] Wandruszka N. Der diagonale Huf. Prakt Tierarzt 2011;92:133–9 ISSN:0032681X.
[67] Page B, Anderson G. Diagonal imbalance of the equine foot: a cause of lameness. In: Proc Am Assoc Equine Pract 38th Annual Convention; 1992. p. 413–18.
[68] Turner TA. The art and frustration of hoof balance. Am Farriers J 2017. accessed 29.07.2022. Available via https://www.americanfarriers.com/ext/resources/images/Marketing/Files/ArtFrustrationOfHoofBalance_web.pdf .